

Ordered States of the Random-Field Model in Three Dimensions

D. A. Garanin and E. M. Chudnovsky

*Physics Department, Lehman College, City University of New York
250 Bedford Park Boulevard West, Bronx, New York 10468-1589, USA*

(Dated: June 5, 2014)

We report numerical investigation of random-field exchange models in three dimensions. The focus is on the vortex-free F-state obtained by the relaxation from the fully ordered initial state. Correlation of energy with the magnetization for models with different numbers of spin components has been studied. Using various hysteresis cycles and minor hysteresis loops, we show that the F-state is significantly more robust for the xy model than it is for the model with the three spin components. Rotation of the F-state reveals memory effects that are pertinent to glasses. We provide insight into the structure of the disordered state by numerically implementing the Imry-Ma argument in which the spins follow the random field averaged over correlated volumes. Thermal stability of the F-state is investigated by Monte Carlo method.

PACS numbers: 74.25.Uv, 75.10.Nr, 02.60.Pn, 64.60.De

I. INTRODUCTION

Recently, it has been argued that the behavior of the order parameter in the random field (RF) model described by the Hamiltonian

$$\mathcal{H} = \int d^d r \left[\frac{\alpha}{2} (\nabla \mathbf{S})^2 - \mathbf{h} \cdot \mathbf{S} \right] \quad (1)$$

is controlled by topology.¹ Here \mathbf{S} is the n -component fixed-length vector field (e.g., spin density of constant length S_0) interacting with the n -component RF $\mathbf{h}(\mathbf{r})$ in d dimensions. At $n > d + 1$ the behavior of the system is fully reversible with the non-ferromagnetic ground state and exponential decay of spin-spin correlations, while at $n \leq d + 1$ the system exhibits glassy behavior with its state determined by the initial condition.¹ In the latter case, the fully ordered initial state relaxes to the state with a finite magnetization that we call the F-state. For the xy model ($n = 2$) in three dimensions the properties of that state have been studied in Ref. 2. In this paper we focus on the comparative study of the F-state in a $3d$ xy model and in a $3d$ Heisenberg model ($n = 3$) with the goal to shed more light on the glassy properties of the RF system.

The problem has a long history. More than forty years ago Larkin, within conceptually similar model, argued that randomly positioned pinning centers destroy translational order in a flux-line lattice.³ Correlations associated with the translational order in flux lattices are of practical interest as they define the size of the vortex bundle that gets depinned by the transport current, which, in turn, determines the critical current.⁴ Related to this effect is a more general qualitative argument suggested by Imry and Ma.⁵ It states that a static RF, regardless of strength, destroys the long-range order associated with a continuous-symmetry order parameter below $d = 4$ spatial dimensions. Aizenman and Wehr^{6,7} provided a mathematical argument that is considered to be a rigorous proof of the Imry-Ma statement. According to this statement the directions

of \mathbf{S} are correlated only within randomly oriented domains of average size $R_f \propto (1/h)^{2/(4-d)}$. Same R_f comes from the Green-function method.⁸ These ideas have been applied to random magnets,^{9–11,13} disordered antiferromagnets,¹⁴ spin-glasses,¹⁵ arrays of magnetic bubbles,¹⁶ superconductors,^{4,17} charge-density waves,¹⁸ liquid crystals,¹⁹ superconductor-insulator transition,²⁰ and superfluid $^3\text{He-A}$ in aerogels.^{21,22}

In early 1980s the renormalization group treatments of the problem by Cardy and Ostlund²³ and by Villain and Fernandez²⁴ questioned the validity of Larkin-Imry-Ma (LIM) argument for distances $R \gtrsim R_f$. The application of scaling and replica-symmetry breaking arguments to statistical mechanics of flux lattices,^{25–35} as well as variational approach,^{36,37} yielded power-law decay of correlations at large distances. These findings suggested that ordering could be more robust against weak static randomness than expected from the LIM theory. Such a quasiordered phase, presumed to be vortex-free in spin systems and dislocation-free in flux lattices, received the name of a Bragg glass. Fisher³⁸ called it an “elastic glass” and argued that the energy associated with vortex loops prevents the xy $3d$ RF system from full disordering.

Numerical evidence of the Bragg/elastic glass has been inconclusive so far. Early numerical work on $1d$ (Ref. 39) and $2d$ (Ref. 40) spin systems with quenched randomness established strong non-equilibrium effects, such as magnetic hysteresis and dependence on initial conditions. Defect-free spin models with relatively large RF and random anisotropy have been studied numerically on small lattices by Fisch.⁴¹ In three dimensions strong non-equilibrium effects have been reported in Refs. 2,42,43. Numerical studies of the $2d$ xy model⁴⁴ revealed that pinning of vortices prevented the system from annihilation of vortex-antivortex pairs and froze it in the vortex glass state. In line with the conjecture made in Ref. 38 it was suggested in Ref. 2 that the high energy cost of vortex loops was preventing the spins in the xy $3d$ RF model from relaxing to a disordered state from the initially ordered state. At elevated temperatures, however, the nu-

merical evidence of the power-law decay of correlations in a $2d$ random-field xy model has been recently obtained by Perret et al.⁴⁵ In the absence of topological defects, the evidence of the logarithmic growth of misalignment with the size of the system has been also found in $2d$ Monte Carlo studies of a crystal layer on a disordered substrate and for pinned flux lattices.^{46,47} Power-law decay of spin-spin correlations has been reported in Monte Carlo studies of the RF Heisenberg model,⁴⁸ as well as for the xy model.⁴⁹ As to real experiments, large areas of defect-free flux lattices have been reported in Ref. 50. The comparison of such experiments with theory, however, is hampered by the fact that for a weak disorder the correlation length in $3d$ can be very large, making it difficult to distinguish large defect-free slightly disordered domains from the Bragg glass.

The paper has the following structure. Some rigorous analytical results that allow us to test the numerics are given in Section II. Energy of the F-state as a function of the magnetization for different number of spin components is obtained in Section IV. Evolution of the F-state generated by a hysteresis cycle is studied in Section V. The dependence of the magnetization of the F-state as function of the strength of the RF is reported in Section VI. Numerical implementation of the Imry-Ma argument is developed in Section VII. Microscopic structure of the F-state is discussed in Section VIII. Memory of the initial condition that results in the rotational elasticity of the F-state is demonstrated in Section IX. Section X deals with the effect of finite temperature on the F-state. Our conclusions are given in Section XI.

II. ANALYTICAL RESULTS

The discrete counterpart of the Hamiltonian (1) that also takes into account Zeeman interaction with the external field \mathbf{H} is given by

$$\mathcal{H} = -\frac{1}{2} \sum_{ij} J_{ij} \mathbf{s}_i \cdot \mathbf{s}_j - \sum_i \mathbf{h}_i \cdot \mathbf{s}_i - \mathbf{H} \cdot \sum_i \mathbf{s}_i, \quad (2)$$

where \mathbf{s}_i is a n -component constant-length ($|\mathbf{s}_i| = s$) spin at the site i of a cubic lattice and \mathbf{h}_i is a quenched RF at that site. The summation is over the nearest neighbors. The factor $1/2$ in the first term is compensating for the double counting of the exchange bonds. In what follows we assume nearest-neighbor exchange. The connection between the parameters of the continuous and discrete models is $\alpha = Ja^{d+2}$, $S_0 = s/a^d$, with a being the lattice spacing.

In this paper we present numerical results on the energy minimization in Eq. (2) for the uncorrelated RF,

$$\langle h_{i\alpha} h_{j\beta} \rangle = \frac{h^2}{n} \delta_{\alpha\beta} \delta_{ij}, \quad (3)$$

(Greek indices being the Cartesian components of the vectors) although computations for a correlated RF have

been performed as well. The correlator above has the same form for the fixed-length RF, $|\mathbf{h}_i| = h = \text{const}$, our main choice, as well as for models with a distributed RF strength h , such as Gaussian distribution. No difference between the fixed-length and Gaussian models has been found in numerical calculations.

Before doing numerical work it is useful to obtain some exact analytical formulas that can provide the ultimate test for our numerical results. One such formula describes the short-range behavior of spin-spin correlations. Choosing in $3d$

$$\mathcal{H}_\lambda = \mathcal{H} - \int d^3r \lambda(\mathbf{r}) \mathbf{S}^2 \quad (4)$$

to account for $\mathbf{S}^2 = S_0^2 = \text{const}$ by the term containing a Lagrange multiplier $\lambda(\mathbf{r})$, one obtains the following extremal equation for \mathbf{S} :

$$\alpha \nabla^2 \mathbf{S} + \mathbf{h} + 2\lambda \mathbf{S} = 0. \quad (5)$$

Multiplying this by \mathbf{S} we have

$$\lambda = -\frac{1}{2S^2} (\alpha \mathbf{S} \cdot \nabla^2 \mathbf{S} + \mathbf{S} \cdot \mathbf{h}) \quad (6)$$

$$\alpha \nabla^2 \mathbf{S} - \frac{\alpha}{S_0^2} \mathbf{S} (\mathbf{S} \cdot \nabla^2 \mathbf{S}) + \mathbf{h} - \frac{1}{S_0^2} \mathbf{S} (\mathbf{S} \cdot \mathbf{h}) = 0. \quad (7)$$

In the second term of Eq. (7)

$$\mathbf{S} \cdot \nabla^2 \mathbf{S} = \nabla (\mathbf{S} \cdot \nabla \mathbf{S}) - (\nabla \mathbf{S})^2 = -(\nabla \mathbf{S})^2 \quad (8)$$

because

$$\mathbf{S} \cdot \nabla \mathbf{S} = \frac{1}{2} \nabla \mathbf{S}^2 = 0. \quad (9)$$

As long as small volumes are studied, this term is quadratic on the perturbation of \mathbf{S} caused by the weak RF, as compared to other terms in Eq. (7) that are linear on \mathbf{h} . Consequently, at small distances this term can be safely dropped. Implicit solution of the remaining equation is

$$\mathbf{S}(\mathbf{r}) = -\frac{1}{\alpha} \int d^3r' G(\mathbf{r}-\mathbf{r}') \left\{ \mathbf{h}(\mathbf{r}') - \frac{\mathbf{S}(\mathbf{r}') [\mathbf{S}(\mathbf{r}') \cdot \mathbf{h}(\mathbf{r}')] }{S_0^2} \right\} \quad (10)$$

with $G(\mathbf{r}) = -1/(4\pi|\mathbf{r}|)$ being the Green function of the $3d$ Laplace equation. Then

$$\begin{aligned} & \frac{1}{2S_0^2} \langle [\mathbf{S}(\mathbf{r}_1) - \mathbf{S}(\mathbf{r}_2)]^2 \rangle = \\ & = \frac{1}{2\alpha^2 S_0^2} \int d^3r' \int d^3r'' [G(\mathbf{r}_1 - \mathbf{r}') - G(\mathbf{r}_2 - \mathbf{r}')] \times \\ & [G(\mathbf{r}_1 - \mathbf{r}'') - G(\mathbf{r}_2 - \mathbf{r}'')] \langle \mathbf{g}(\mathbf{r}') \cdot \mathbf{g}(\mathbf{r}'') \rangle, \end{aligned} \quad (11)$$

where $\mathbf{g} \equiv \mathbf{h} - \mathbf{S}(\mathbf{S} \cdot \mathbf{h})/S_0^2$.

Neglecting the weak correlation between \mathbf{h} and \mathbf{S} , with the help of the continuous equivalent of Eq. (3),

$$\langle h_\alpha(\mathbf{r}') h_\beta(\mathbf{r}'') \rangle = \frac{h^2}{n} \delta_{\alpha\beta} \delta(\mathbf{r}' - \mathbf{r}''), \quad (12)$$

one obtains

$$\langle g_\alpha(\mathbf{r}')g_\beta(\mathbf{r}'') \rangle = \frac{h^2}{n} \left(\delta_{\alpha\beta} - \frac{\langle S_\alpha S_\beta \rangle}{S_0^2} \right) a^3 \delta(\mathbf{r}' - \mathbf{r}''). \quad (13)$$

Consequently

$$\langle \mathbf{g}(\mathbf{r}') \cdot \mathbf{g}(\mathbf{r}'') \rangle = \frac{h^2}{n} (n-1) a^3 \delta(\mathbf{r}' - \mathbf{r}''). \quad (14)$$

This gives

$$\begin{aligned} \frac{1}{2S_0^2} \langle [\mathbf{S}(\mathbf{r}_1) - \mathbf{S}(\mathbf{r}_2)]^2 \rangle &= \\ &= \frac{h^2 a^3}{2\alpha^2 S_0^2} \left(1 - \frac{1}{n} \right) \int d^3 r [G(\mathbf{r}_1 - \mathbf{r}) - G(\mathbf{r}_2 - \mathbf{r})]^2 \\ &= \frac{h^2 a^3}{8\pi\alpha^2 S_0^2} \left(1 - \frac{1}{n} \right) |\mathbf{r}_1 - \mathbf{r}_2| = \frac{|\mathbf{r}_1 - \mathbf{r}_2|}{R_f} \end{aligned} \quad (15)$$

with¹

$$\frac{R_f}{a} = \frac{8\pi\alpha^2 S_0^2}{h^2 a^4 (1 - 1/n)} = \frac{8\pi}{(1 - 1/n)} \left(\frac{Js}{h} \right)^2. \quad (16)$$

The weakness of the RF should be measured against the exchange field $6Js$ created in a $3d$ cubic lattice by the nearest neighbors of each spin. This can be seen by representing Eq. (16) in the form

$$\frac{R_f}{a} = \frac{2\pi}{9(1 - 1/n)} \left(\frac{6Js}{h} \right)^2, \quad (17)$$

with the numerical factor in front of $(6Js/h)^2$ of order unity, e.g., $2\pi/6$ for $n = 3$.

Noticing that

$$\frac{1}{2S_0^2} \langle [\mathbf{S}(\mathbf{r}_1) - \mathbf{S}(\mathbf{r}_2)]^2 \rangle = 1 - \frac{1}{S_0^2} \langle \mathbf{S}(\mathbf{r}_1) \cdot \mathbf{S}(\mathbf{r}_2) \rangle \quad (18)$$

we finally obtain

$$\langle \mathbf{s}_i \cdot \mathbf{s}_j \rangle = s^2 \left(1 - \frac{|\mathbf{r}_i - \mathbf{r}_j|}{R_f} \right). \quad (19)$$

for the short range correlations. This formula is in agreement with the famous Larkin's result,³ with Eq. (16) providing the correlation length for arbitrary n .

Long-range correlations are difficult to obtain by the above Green-function method because of the high non-linearity of Eq. (7). However, the case of $n = \infty$ permits exact analytical solution at all distances due to its equivalence⁵¹ to the mean-spherical model in which only the volume average of \mathbf{S}^2 rather than the local \mathbf{S}^2 is a constant, $V^{-1} \int d^3 r \mathbf{S}^2 = S_0^2$. In this case λ in Eq. (5) is a constant that we will write as $\lambda = -\alpha k/2$. Then extremal equation for \mathbf{S} is linear

$$(\nabla^2 - k^2)\mathbf{S} = -\frac{1}{\alpha}\mathbf{h} \quad (20)$$

with a general solution

$$\mathbf{S}(\mathbf{r}) = -\frac{1}{\alpha} \int d^3 r' G_k(\mathbf{r} - \mathbf{r}') \mathbf{h}(\mathbf{r}'), \quad (21)$$

$G_k(\mathbf{r}) = -e^{-k|\mathbf{r}|}/(4\pi|\mathbf{r}|)$ and $G_k(\mathbf{q}) = -1/(q^2 + k^2)$ being the Green function of Eq. (20) and its Fourier transform, respectively. Consequently,

$$\begin{aligned} \langle \mathbf{S}(\mathbf{r}_1) \cdot \mathbf{S}(\mathbf{r}_2) \rangle &= \frac{1}{\alpha^2} \int d^3 r d^3 r' G_k(\mathbf{r}_1 - \mathbf{r}') G_k(\mathbf{r}_2 - \mathbf{r}'') \\ &\times \langle \mathbf{h}(\mathbf{r}') \cdot \mathbf{h}(\mathbf{r}'') \rangle = \frac{h^2 a^3}{\alpha^2} \int d^3 r G_k(\mathbf{r} - \mathbf{r}_1) G_k(\mathbf{r} - \mathbf{r}_2) \\ &= \frac{h^2 a^3}{\alpha^2} \int \frac{d^3 q}{(2\pi)^3} \frac{e^{i\mathbf{q} \cdot (\mathbf{r}_1 - \mathbf{r}_2)}}{(q^2 + k^2)^2} = \frac{h^2 a^3}{8\pi\alpha^2 k} e^{-k|\mathbf{r}_1 - \mathbf{r}_2|}. \end{aligned} \quad (22)$$

Writing the correlation function in the form $\langle \mathbf{S}(\mathbf{r}_1) \cdot \mathbf{S}(\mathbf{r}_2) \rangle = S_0^2 \exp(-|\mathbf{r}_1 - \mathbf{r}_2|/R_f)$, we finally obtain $k = 1/R_f$,

$$\langle \mathbf{s}_i \cdot \mathbf{s}_j \rangle = s^2 \exp \left(-\frac{|\mathbf{r}_i - \mathbf{r}_j|}{R_f} \right) \quad (23)$$

where

$$\frac{R_f}{a} = \frac{8\pi\alpha^2 S_0^2}{h^2 a^4} = 8\pi \left(\frac{Js}{h} \right)^2. \quad (24)$$

This result is in agreement with Eqs. (16) and (19) at $n = \infty$.

III. NUMERICAL METHOD

Random-field systems demonstrate glassy states with many local energy minima. As in Ref. 2, at $T = 0$ we minimize the energy of the system by the method of relaxation starting from typical initial conditions such as random and collinear. The method consists in sequentially rotating spins towards the direction of the effective field at the given site with the probability α and flipping the spins over the effective field with probability $1 - \alpha$. The former was used as the only method in Ref. 40. The latter is the so-called over-relaxation that conserves the energy. Thus α has a meaning of the relaxation constant. For our glassy systems the method works most efficiently for small α . Most of the results were obtained with $\alpha = 0.03$. The resulting energy minima are representative local energy minima, while no attempt to directly search for the global energy minimum was done. The latter would require a different method and usually does not have much sense because the global energy minimum may be practically unreachable due to high energy barriers.

At nonzero temperatures we replace rotating spins towards the direction of the effective field by regular Monte Carlo updates, keeping the over-relaxation dominating via the same small value of α .

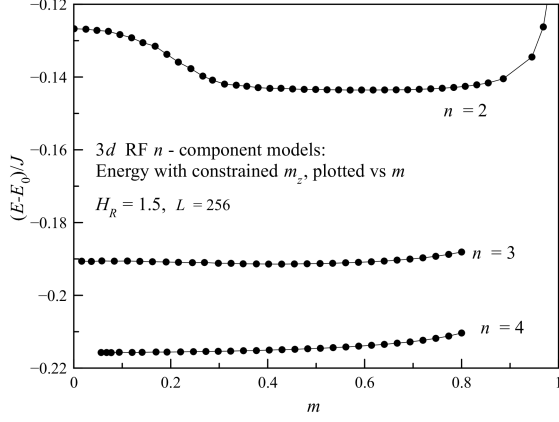


Figure 1: Energy E vs the magnetization m for different numbers of spin components n . Each point was obtained by relaxation from a random initial state.

In numerical work we consider a simple cubic lattice with periodic boundary conditions and use H_R as h , setting $s = a = J = 1$. The numerical method has been implemented in Wolfram Mathematica in a compiled and parallelized form. To reduce statistical fluctuations in our random system, one can do averaging over realizations of the random field. A better way is to use systems of large sizes because of self-averaging over the system. Another argument for using large sizes is the requirement $R_f \ll L$, where L is system size in atomic units. For weak random field h , Eq. (16) gives a large R_f so that a large L is needed to prove ordering or disordering. For $R_f \gtrsim L$ the system has a large finite-size magnetization in all cases.

Vorticity in the xy model can be computed by considering rotations of spins when one is moving in the positive direction (counter-clockwise) around each square plaquette within xy , yz , and zx planes.^{2,42} If the spins rotate by zero angle, there is no singularity. Rotation by $\pm 2\pi$ corresponds to vortex/antivortex. For models with the number of spin components this method cannot be used to detect singularities. Thus we use the following method. In 3d, for each cube of neighboring spins the average spin vector and its length is computed. If the latter is smaller than a preset value (we used 0.5), there is a singularity at this point. The fraction of positions having singularities is reported as f_S . This method works well for any lattice dimensions and number of spin components. For the xy model it yields the results consistent with those obtained by looking for vortices/antivortices.

IV. ENERGY AND MAGNETIZATION

The question of correlation of the energy of local energy minima with the magnetization in the xy model has been studied in Ref. 2 and the results for some representative local energy minima have been presented. The energy of the vortex-glass (VG) state was found to correlate per-

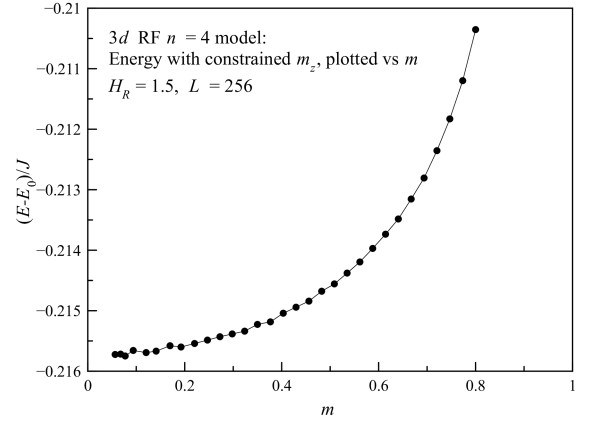
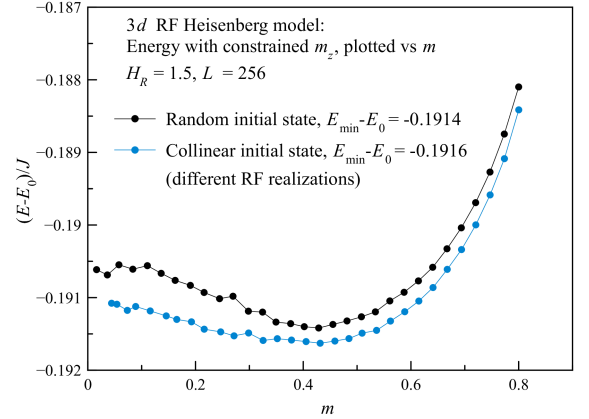
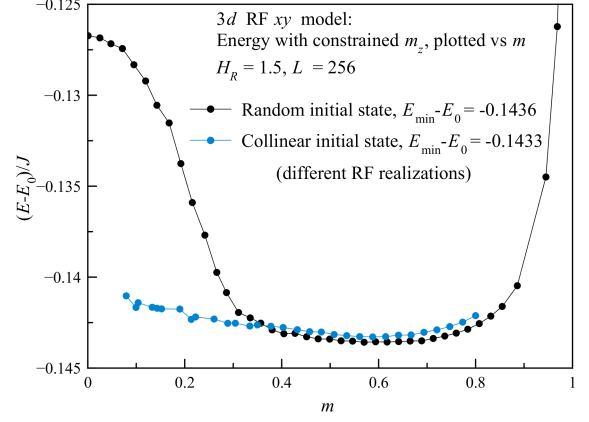


Figure 2: Energy E vs the magnetization m for different models. Each point was obtained by relaxation from a random or collinear initial state.

fectly with the vorticity and to be higher than the energy of the F-state. The latter had a flat minimum at m between 0.5 and 0.6 for $H_R/J = 1.5$. The F-states with lower magnetization (the lowest is just below $m = 0.2$) have manifestly higher energies.

Here a slightly different computation was performed for models with different n . The energy was minimized with the constraint of $m_z = \text{const}$ applying a self-

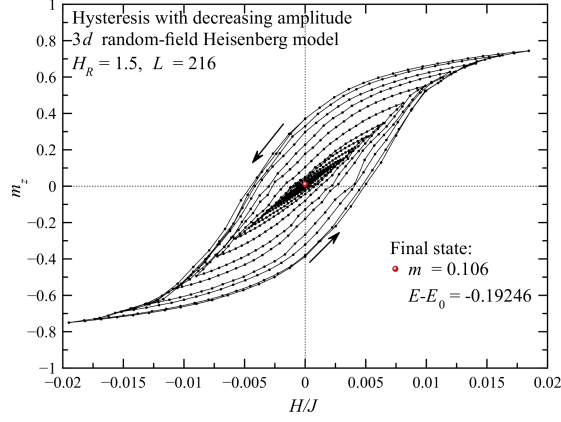


Figure 7: Magnetization evolution of the 3d Heisenberg model in the hysteresis loop with the amplitude decreasing to zero.

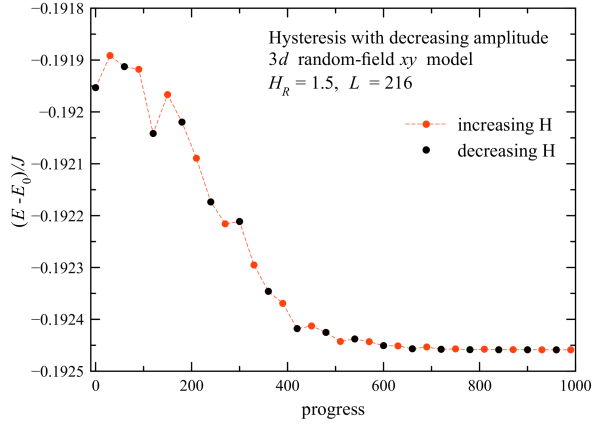


Figure 8: Energy evolution of the 3d Heisenberg model in the hysteresis loop with decreasing amplitude. Only points corresponding to $H = 0$ are shown. Black (red) circle correspond to decreasing (increasing) H .

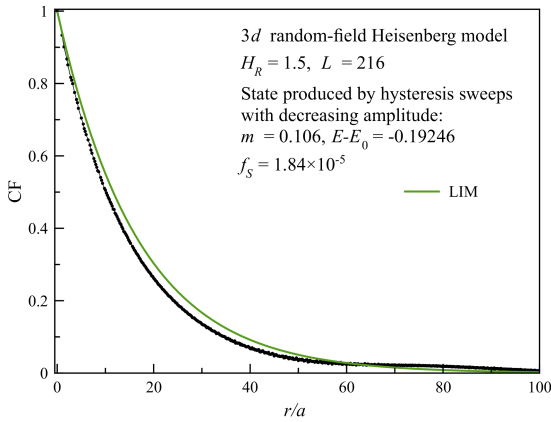


Figure 9: Spin correlation function of the 3d Heisenberg model at the end of the hysteresis-with-decreasing-amplitude cycle.

illustrates the existence of F-states with different magnetization values.

Making repeated hysteresis loops with the amplitude of the applied field H decreasing to zero, one can hope to end up in a state of a smaller energy. To save time, the process can be started as free relaxation in zero field from a collinear state aligned with the direction in which H will be applied. This results in the F-state. Then the field is increased in the direction opposite to the initial magnetization etc. For the 3d xy model, starting with a large hysteresis amplitude leads to the rupture of spin walls and creating vortex loops. As the result, the system ends up in a state of a higher energy than the initial F state.

What can be done for the 3d xy model is to lower the energy of the initial F-state by making hysteresis loops with the initial amplitude smaller than the magnetic field causing rupture of spin walls. The evolution of the magnetization in this sequence vs the applied field is shown in Fig. 4. Evolution of the energy in this sequence is shown in Fig. 5 (zero values of H only). One can see that the final energy is indeed lower than the initial energy $(E - E_0)/J = -0.1439$ of the state with $m = 0.676$ obtained by relaxation from the collinear state (the first point in Fig. 5). For $H_R/J = 1.5$ and $L = 256$ the final state has $m = 0.562$ and $(E - E_0)/J = -0.14425$. Another computation with $H_R/J = 1.5$ and $L = 216$ resulted in $m = 0.567$ and $(E - E_0)/J = -0.1441$. It is important to notice that the amplitude of the hysteresis loop remains small enough so that rupture of spin walls accompanied by the creation of vortex loops⁴³ does not happen. Otherwise the process would lead to the energy increase: the final state (also having the large magnetization typical for the F-state) contains singularities and its energy is higher than that of the F-state obtained by relaxation from the collinear state. These experiments show that the F-state of the 3d xy model is robust, one can optimize but not easily destroy it.

Completely different behavior has been observed for the 3d Heisenberg model. Here, as shown in Fig. 6, decreasing the magnetic field to negative values immediately leads to the formation of singularities - hedgehogs. Thus hedgehogs are unavoidable and one can start with a larger amplitude of the field sweep encompassing the being practically zero and $m = 0.106$. Such a small magnetization can be explained by the finite-size effect in the absence of ordering. Disappearance of the magnetization is accompanied by the decrease of the energy in Fig. 8 down to $(E - E_0)/J = -0.19246$. The fraction of singularities in the final state is $f_S = 1.84 \times 10^{-5}$. One can see that for the 3d Heisenberg model the energy increase due to the creation of singularities in the course of aligning of spins with the RF is smaller than the energy gain due to the aligning. Although relaxation from a collinear state stops at a finite m because of the singularities, the more sophisticated process of the magnetic field sweep with decreasing amplitude helps the system to disorder. The spin correlation function in the final disordered state

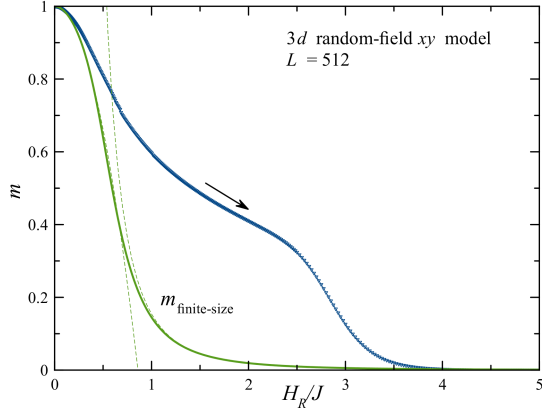


Figure 10: Magnetization vs the random field strength H_R for the 3d xy model, $L = 512$. Green line is the finite-size magnetization expected in the absence of ordering. Dashed green lines are Eqs. (25) and (27).

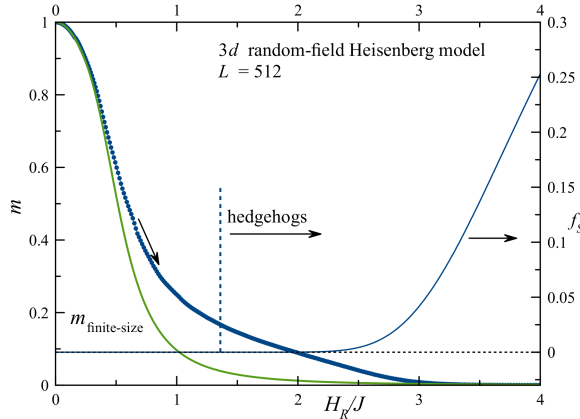


Figure 11: Magnetization vs the random field strength H_R for the Heisenberg model, $L = 512$. Green line is the finite-size magnetization expected in the absence of ordering.

shown in Fig. 9 is close to the LIM exponential form. Slightly lower correlations in the numerical result can be explained by hedgehogs.

VI. MAGNETIZATION OF THE F-STATE VS RANDOM-FIELD STRENGTH

Another way to obtain the F-states is, starting from a collinear state, to increase the strength of the random field H_R from zero in small steps.² This procedure leads to the F-states with a smaller magnetization than that obtained directly by the relaxation from a collinear state. Results for magnetization and energy for the 3d xy model at $H_R/J = 1.5$ are $m = 0.467$ and $(E - E_0)/J = -0.14425$. New computation for $H_R/J = 1.5$ and $L = 512$, Figs. 10, 11, and 12, yields

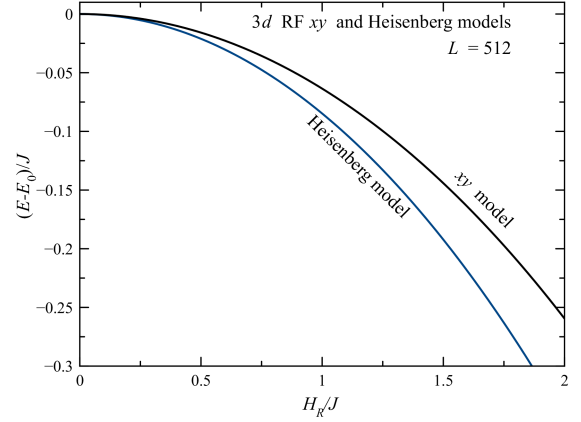


Figure 12: Energy vs the random field strength H_R for the xy and Heisenberg models, $L = 512$.

$m = 0.486$ and $(E - E_0)/J = -0.14415$ for the xy model and $m = 0.146$ and $(E - E_0)/J = -0.19226$ for the Heisenberg model. Comparison of these results with those above shows that the energy landscape of the RF model is very flat and states with markedly different magnetizations have very close energies.

The computed magnetization should be compared with the finite-size magnetization expected in the absence of ordering in the intermediate range of H_R . The latter can be obtained analytically in the regions $R_f \gg L$ and $R_f \ll L$, where the magnetic correlation range R_f is given by Eq. (16) and $h \equiv H_R$. For small H_R one has $R_f \gg L$ and the short-range order extends over the whole system, making the magnetization $m \cong 1$. Deviations from this short-ordered state can be found perturbatively and for the cube of size L with periodic boundary conditions the result has the form

$$m \cong 1 - A \frac{L}{R_f} \cong \left(1 + A \frac{L}{R_f}\right)^{-1}, \quad (25)$$

where

$$A = \frac{1}{4\pi^3} \sum_{n_{x,y,z}=-\infty}^{\infty} \frac{1}{(n_x^2 + n_y^2 + n_z^2)^2} \simeq 0.1333 \cong \frac{4}{30}. \quad (26)$$

In the case $R_f \ll L$, assuming the exponential spin correlation function of Eq. (23) that has been derived analytically for $n = \infty$ in Section II and confirmed numerically¹ for 3d models with $n > d + 1$ one obtains²

$$m \cong \sqrt{8\pi} \left(\frac{R_f}{L}\right)^{3/2} \quad (27)$$

(the so-called “fluctuational” or finite-size magnetization). One can build a good interpolation formula in the whole range of R_f that reads

$$m = \frac{1}{\sqrt{1/m_1^2 + 1/m_2^2}}, \quad (28)$$

m_1 and m_2 being the two limiting expressions above, Eqs. (25) and (27).

One can see that for the 3d xy model in Fig. 10 the computed magnetization is substantially larger than the finite-size magnetization given by Eq. (28) in the intermediate range of H_R . For small H_R the system is short-range-ordered, $m \cong 1$. For large H_R spins are forced to align with the random field and the system is completely disordered. The quasi-plateau of $m(H_R)$ followed by the shoulder at $H_R/J \simeq 2.5$ is due to the effect of vortex loops. As further decrease of m requires creating vortex loops that cost energy, the system remains ordered.¹ This holds until the the random field overpowers the exchange.

An interesting fact is the reversibility of the $m(H_R)$ curve (in a limited range of H_R) that contrasts the hysteresis of $m(H)$ characterized by Barkhausen jumps. Increasing H_R leads to turning spins more and more in the direction of the random field without overcoming any barriers. This suggests that the obtained state is generically related to the collinear ground state of a pure ferromagnet. Reaching $H_R/J \simeq 2$ causes creation of vortex loops and reversibility of the $m(H_R)$ curve breaks down. Thus the F-states obtained by adiabatic increasing of H_R are distinguished among all the F-states and they likely to have the lowest energy among them.

Corresponding results for the 3d Heisenberg model ($n = 3$) shown in Fig. 11 reveal a much smaller magnetization of the adiabatic F-state than for the xy model ($n = 2$). Even for the system size as large as $L = 512$, the computed magnetization is not much greater than the finite-size magnetization. This is because the F-state in the Heisenberg model is topologically protected by hedgehogs having much smaller energy than vortex loops of the xy model. Still, the nearly constant slope of $m(H_R)$ in the region $1 \lesssim H_R/J \lesssim 3$ indicates the existence of the ordered state that is slowly destroyed by emerging singularities – hedgehogs. The fraction of hedgehogs f_S is shown on the right axis of Fig. 11.

VII. NUMERICAL IMPLEMENTATION OF THE IMRY-MA ARGUMENT

Imry and Ma (IM) argument⁵ assumes that in RF models the spins are directed along the random field averaged over correlated volumes of linear size R , found self-consistently by minimizing the energy due to the random field and exchange. The energy per spin is estimated as

$$E - E_0 \sim -sh \left(\frac{a}{R} \right)^{d/2} + s^2 J \left(\frac{a}{R} \right)^2, \quad (29)$$

where E_0 is the energy per spin of a collinear state. The first term in this formula is the statistical average of the RF energy in the IM domain of size R while the second term is the exchange energy from smooth rotation of the magnetization between adjacent domains. Minimization

of the energy with respect to R yields $R = R_f$, where

$$R_f \sim a \left(\frac{sJ}{h} \right)^{2/(4-d)}. \quad (30)$$

For $d = 3$ it coincides with Eq. (16), however, without the dependence on n . The resulting energy of the IM state is

$$E - E_0 \sim -s^2 J \left(\frac{h}{sJ} \right)^{4/(4-d)} \quad (31)$$

that yields $E - E_0 \sim -h^4/J^3$ in a 3d field model. It can be shown¹ that the IM state of the 3d xy model inevitably contains vortex loops that cost energy. The resulting estimation for the energy of the IM state then becomes²

$$E - E_0 \sim \frac{h^4}{s^2 J^3} \frac{1}{\ln^3(sJ/h)}. \quad (32)$$

In the case of a weak random field the large logarithm in the denominator significantly decreases the energy gain due to the adjustment of spins to the averaged random field.

In the lattice model the main contribution to the adjustment energy arises at the atomic scale and is given by $E - E_0 \sim -h^2/J$ in all dimensions. The IM energy represents small correction to that energy due to the large-scale rotation of the magnetization on a large distance R_f . Finite value of R_f for any $d < 4$ supports the IM picture of a disordered state. However, it does not prove rigorously that the ground state of the system has $m = 0$. To prove that one has to compare the energy of the $m = 0$ state, that may contain topological defects, with the energy of defect-free F-states with $m \neq 0$.

Mathematical implementation of the averaged random field is

$$\bar{\mathbf{h}}_i = \sum_j K_{ij} \mathbf{h}_j, \quad (33)$$

or, within the continuous approximation,

$$\bar{\mathbf{h}}(\mathbf{r}) = \int d^d \mathbf{r}' K(r') \mathbf{h}(\mathbf{r}' + \mathbf{r}), \quad (34)$$

where K an averaging kernel. Spins follow the direction of $\bar{\mathbf{h}}$ and have to be normalized,

$$\mathbf{s}(\mathbf{r}) = s \frac{\bar{\mathbf{h}}(\mathbf{r})}{|\bar{\mathbf{h}}(\mathbf{r})|}. \quad (35)$$

The choice of the averaging kernel introduces uncertainty into the IM construction. Possible choices for $K(r)$ are rigid sphere, rigid cube, Gaussian, exponential, etc.

For the δ -correlated random field, Eqs. (3) or (12), the correlator of the averaged random field is given by

$$\langle \bar{h}_\alpha(\mathbf{r}) \bar{h}_\beta(\mathbf{r}') \rangle = \frac{h^2}{n} \delta_{\alpha\beta} \Gamma(|\mathbf{r} - \mathbf{r}'|), \quad (36)$$

where

$$\Gamma(r) = \frac{1}{a^d} \int d^d \mathbf{r}' K(r') K(|\mathbf{r} - \mathbf{r}'|). \quad (37)$$

Thus the averaged random field is a correlated random field. We will require $\Gamma(0) = 1$ that yields the condition

$$1 = \frac{1}{a^d} \int d^d \mathbf{r} K^2(r). \quad (38)$$

Choosing different $K(r)$, one can obtain different $\Gamma(r)$. Considering, instead of Eq. (35), spin vectors

$$\mathbf{s}(\mathbf{r}) = s \frac{\bar{\mathbf{h}}(\mathbf{r})}{h} \quad (39)$$

that are normalized on average amounts to the mean spherical model (see Sec. II). The correlation function of these spins is exactly $\Gamma(r)$. The actual spins, however, have to be normalized at each site by Eq. (35). The denominator in Eq. (35) introduces singularities in the spin field where $|\bar{\mathbf{h}}(\mathbf{r})| = 0$. This happens forcibly, if the number of spin components n is small enough, $n \leq d$, that includes practical cases.¹ For $n > d$ there is no topological reason for $|\bar{\mathbf{h}}(\mathbf{r})| = 0$, and one can expect that the difference between the spin fields defined by Eqs. (35) and (39) is small.

Let us consider particular averaging kernels. The rigid-cube kernel satisfying Eq. (38) is given by

$$K(\mathbf{r}) = \begin{cases} [a/(2R)]^{d/2}, & |x|, |y|, |z| \leq R \\ 0 & |x|, |y|, |z| > R. \end{cases} \quad (40)$$

The correlation function Γ is defined by the overlap area of two shifted cubes that leads to the small-distance behavior

$$1 - \Gamma(r) \sim r/R. \quad (41)$$

Disappearance of the overlap leads to the vanishing of Γ at finite distances, an undesirable property.

The Gaussian averaging kernel in $3d$ is given by

$$K(r) = \left(\frac{2}{\sqrt{\pi}} \frac{a}{R} \right)^{3/2} e^{-2(r/R)^2}. \quad (42)$$

The corresponding RF correlation function is

$$\Gamma(r) = e^{-(r/R)^2}. \quad (43)$$

One can see that this result disagrees with the spin-spin correlation function that follows from the Green-function method, in particular, with Eq. (23) for the mean spherical model.

The exponential averaging kernel in $3d$ is given by

$$K(r) = \frac{1}{\sqrt{\pi}} \left(\frac{a}{R} \right)^{3/2} e^{-r/R}. \quad (44)$$

The corresponding RF correlation function is non-exponential. It goes quadratically at small distances,

$$\Gamma(r) \cong 1 - \frac{1}{6} \left(\frac{r}{R} \right)^2, \quad r \ll R \quad (45)$$

again contradicting and has the long-distance behavior

$$\Gamma(r) \cong \frac{1}{3} \left(\frac{r}{R} \right)^2 e^{-r/R}, \quad R \ll r, \quad (46)$$

again, contradicting Eq. (23).

On the contrary, Yukawa averaging kernel in $3d$

$$K(r) = \frac{a^{3/2}}{\sqrt{2\pi} R} \frac{1}{r} e^{-r/R} \quad (47)$$

that has the same singularity as the Green function of the mean-spherical model ($n = \infty$), leads to the desired exponential correlation function of the correlated RF

$$\Gamma(r) \cong e^{-r/R} \quad (48)$$

and thus of the spin correlation function for spins normalized on average. This is not a surprise because for the Yukawa kernel Eqs. (34) and (39) are equivalent to Eq. (21) that results in Eq. (23).

Let us consider the energies of the constructed IM states, using the simplified form of the spin field given by Eq. (39). Then $\Gamma(r)$ above is the spin-spin correlation function. The exchange energy is defined by the nearest-neighbor correlation function, thus

$$E_{\text{ex}} - E_0 = s^2 dJ [1 - \Gamma(a)], \quad (49)$$

where $E_0 = dJ$ is the ground-state energy of a pure magnet. This method of computing the exchange energy used in Ref. 2 ignores lattice-discreteness effects at small distances. However, it can be shown that the error is very small. One can see that $E_{\text{ex}} - E_0 \propto 1/R$ for the rigid cut-off and Yukawa averaging kernels and $E_{\text{ex}} - E_0 \propto 1/R^2$ for the Gaussian and exponential averaging kernels. As the second case is in accord with the IM argument, this type of kernels will be called regular.

The random-field energy per spin is given by $E_{RF} = -\langle \mathbf{s}_i \cdot \mathbf{h}_i \rangle$. Using Eq. (39), one obtains

$$\begin{aligned} E_{RF} &= -\frac{s}{h} \langle \bar{\mathbf{h}}_i \cdot \mathbf{h}_i \rangle = -\frac{s}{h} \left\langle \sum_j K_{ij} \mathbf{h}_j \cdot \mathbf{h}_i \right\rangle \\ &= -sh K_{ii} = -sh K(0). \end{aligned} \quad (50)$$

For regular kernels as well as for the rigid cut-off kernel in $3d$, using Eqs. (42) and (44), one obtains $E_{RF} \propto -1/R^{3/2}$, as in the IM argument. In fact, there is an agreement of both exchange and random-field energies with their IM forms for any dimension d , if regular averaging kernels are used. Minimizing the total energy with respect to R , one obtains the value of R_f above and the minimal energy $E - E_0 \propto -h^4/J^3$ in $3d$, according to Eq. (31). Thus, regular averaging kernels fully reproduce the

original IM argument⁵ and provide its implementation with the results differing only by a numerical factor.

However, using regular kernels misses the main contribution to the energy due to adjustment of spins at the atomic scale, $E - E_0 \propto -h^2/J$.² Another drawback of these kernels is the wrong spin correlation function in 3d.

For the Yukawa averaging kernel, Eq. (50) is singular within the continuous approximation. However, the lattice Green function with coinciding indices is finite. The regularization can be done by the replacement $r \rightarrow a$ in the denominator of Eq. (47). The corresponding modification yields

$$K_{ii} = \eta \sqrt{\frac{a}{2\pi R}}, \quad (51)$$

where η is a constant. The total energy for the Yukawa averaging kernel following from Eqs. (48), (49), (50) and the formula above in 3d is given by

$$E - E_0 = 3s^2 J \frac{a}{R} - sh\eta \sqrt{\frac{a}{2\pi R}}. \quad (52)$$

Minimizing this energy over R yields

$$\frac{R_f}{a} = 8\pi \left(\frac{3J}{\eta h} \right)^2 \quad (53)$$

and

$$E_{\text{ex}} - E_0 = \frac{\eta^2 h^2}{24\pi J}, \quad E_{RF} = -2(E_{\text{ex}} - E_0). \quad (54)$$

Choosing $\eta^2 = 9(1 - 1/n)$, one recovers R_f of Eq. (30) and the total adjustment energy

$$E - E_0 = - \left(1 - \frac{1}{n} \right) \frac{3h^2}{8\pi J} \quad (55)$$

that for the xy model ($n = 2$) has been calculated in Ref. 2. Summarizing, using the Yukawa averaging kernel in the IM construction provides correct forms of the spin correlation function, including the magnetic correlation length R_f , as well as the leading contribution to the energy h^2/J . To the contrary, the so-called “long-range” energy of the IM argument does not arise. In the limit $n \rightarrow \infty$ the results above become exact and coincide with those of the mean spherical model.

Below the numerical results will be presented. The rigid-cube kernel is most convenient for computation. Spin-spin correlation function for the state with $R = R_{IM} = 100$ is shown in Fig. VII. It has a characteristic shape with a nearly-constant slope ending at the distance $2R$. This shape is very different from the IM exponential correlation function that follows from the Green function method. Starting from this constructed IM state, numerical minimization of the energy with $H_R/J = 1.5$ was performed. The resulting spin-spin correlation function also shown in the figure coincides with the IM curve and

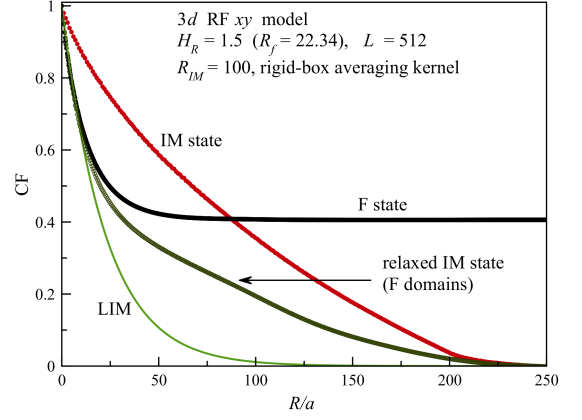


Figure 13: Spin correlation function of the constructed IM state with the rigid-cube cut-off and of the corresponding relaxed state. The spin-spin correlation function of the F-state and the theoretical LIM curve are shown for comparison.

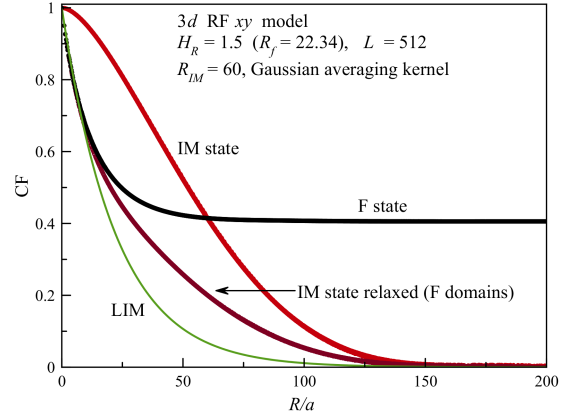


Figure 14: Spin-spin correlation function of the constructed IM state with the Gaussian averaging kernel and of the corresponding relaxed state. The spin-spin correlation function of the F-state and the theoretical LIM curve are shown for comparison.

with the correlation function of the F-state at the distances $r \lesssim R_f$, where $R_f/a = 22.34$. At larger distances this correlation function is decreasing slowly, similarly to the constructed IM correlation function, and it turns to zero at the same distance. This result implies that at distances $r \lesssim R_f$ the system relaxes to minimize its energy, whereas at larger distances the system is pinned by the RF and its state depends on the initial state. Similar results were obtained with the Gaussian averaging kernel, see Fig. 14. Energies of the relaxed IM states in both figures above are slightly greater than the energy of the F-state. This means that long-distance correlations can be changed at a very small energy cost, similarly to creating a domain wall in a big system.

The results for the IM construction with the Yukawa

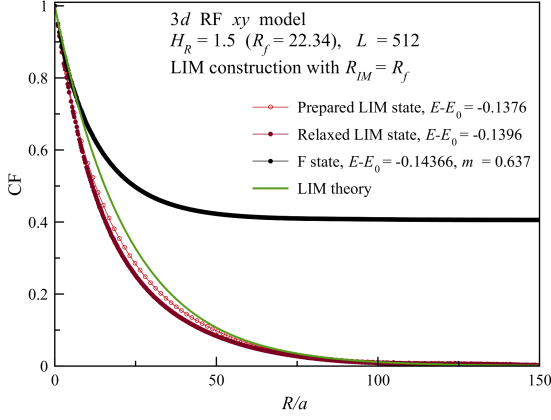


Figure 15: Spin-spin correlation function of the constructed IM state with the Yukawa averaging kernel and of the corresponding relaxed state. The spin-spin correlation function of the F-state and the exponential LIM curve are shown for comparison.

averaging kernel for the 3d xy model are shown in Fig. 15. Here also $H_R/J = 1.5$ was used, and the constructed state was created with the actual spin correlation range $R_f/a = 22.34$. Since spins are normalized by Eq. (35) this creates singularities, the spin-spin correlation function goes slightly below the LIM curve, as can be seen in Fig. 15. Subsequent relaxation makes the correlation function go slightly lower than the IM curve. The energies of both, the constructed IM state and the corresponding relaxed state, are close to that of the F-state but still higher. This is because the constructed IM state and the relaxed state possess vortex loops that cost energy.

VIII. MICROSCOPIC STRUCTURE OF THE F-STATE

For arbitrary number of spin components n the correlation range R_f of the RF system perfectly agrees with the value calculated by the Green-function method, that is itself in a qualitative agreement with the Imry-Ma argument. For any n the spin-spin correlation function decreases as $C(r) \cong 1 - r/R_f$ at distances $r \lesssim R_f$. At $n > d + 1$ correlations decay exponentially regardless of the initial condition for the spins.¹ However, for $n \leq d$ at $r > R_f$ the correlation function of the state obtained by the relaxation from the fully ordered state has a plateau corresponding to a non-zero magnetization. The spin field in the F-state does not have singularities that would arise in the case of $n \leq d$ in the hypothetical Imry-Ma state in which spins follow the RF averaged inside the IM domains of linear size R_f .

It is interesting to look at the difference between the F-state and the IM state by visualising the domains. For this purpose, color labeling of the F-states in the 2d xy

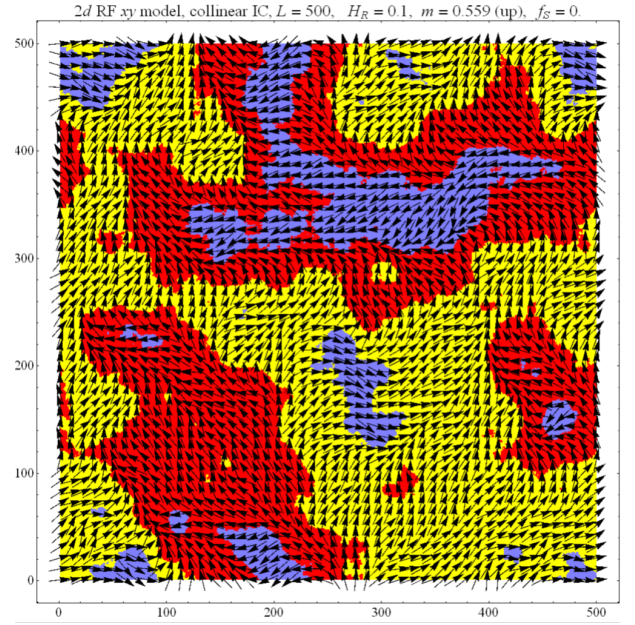


Figure 16: Imry-Ma domains in the F-state of 2d xy model

model has been done as shown in Fig. 16. With the sample's magnetization pointing up (positive y direction), regions with spins turned to the right are coded yellow and spins turned to the left are coded red. Spins directed down are labeled blue overriding yellow and red. The results can be understood as follows. Under the influence of the random field spins are rotating clockwise and counterclockwise from the initial direction up, becoming yellow and red. Rotating more into the down region, they become blue. In this scenario, blue regions are entirely inside their parent yellow and red regions and spins are divided into rotated clockwise and counterclockwise. This spin state is topologically equivalent to the initial collinear state and can be transformed back to it without creating or annihilating topological structures.

Color-coded regions in Fig. 16 can be interpreted as IM domains. Boundaries between yellow and red correspond to $s_x = 0$, whereas the boundaries between yellow and blue or between red and blue correspond to $s_y = 0$. As was shown in Ref. 2 the IM construction inevitably leads to the formation of vortices or anti-vortices on purely mathematical grounds. This does not happen when spins rotate clockwise or counterclockwise to form the F-state. In that state the spins do not follow the averaged random field precisely and the system disorders only partially, keeping the memory of the initial collinear state. Complete disordering is blocked because singularities would increase the system's energy.

If blue regions corresponding to the down spins rotated clockwise and counterclockwise merge, as can be seen near the bottom of Fig. 17, there would be an intersection of the yellow-red boundary with the red-blue and yellow-blue boundaries, that is, an intersection of the $s_x = 0$ and $s_y = 0$ lines. As the result, there is a

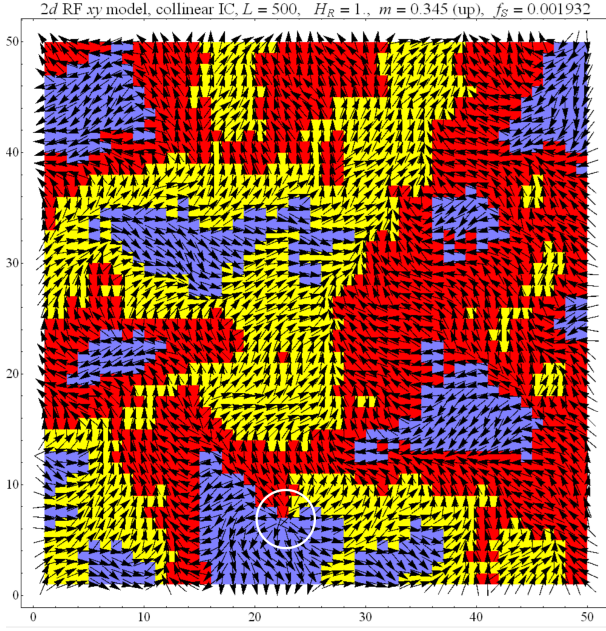


Figure 17: Imry-Ma domains in the F-state of $2d\ xy$ model, with a vortex in the lower part inside the white circle.

white-encircled vortex in Fig. 17. Singularities, such as vortices, can be created by a strong enough random field out of a collinear state, as is the case in Fig. 17. One can see that the state shown in Fig. 17 has lost the memory of the initial collinear state and it cannot be returned to it without changing topology.

One can suggest the form of the IM argument that does not assume a complete disordering and is thus suitable for the description of F-states.² It takes into account the adjustment of spins to the random field at all length scales. Groups of spins of linear size R rotate by an adjustment angle ϕ (considered as small to begin with) under the influence of the components of the averaged random field perpendicular to the initial direction. The corresponding energy per spin is given by

$$E - E_0 \sim -sh \left(\frac{a}{R} \right)^{d/2} \phi + s^2 J \left(\frac{a}{R} \right)^2 \phi^2. \quad (56)$$

Minimizing this expression with respect to ϕ , one obtains

$$\phi \sim \left(\frac{R}{R_f} \right)^{(4-d)/2}, \quad (57)$$

where R_f is given by Eq. (30). The angular deviation increases with the distance and becomes large at $R \sim R_f$. The energy per spin corresponding to spin adjustment at the distance R can be obtained by substituting Eq. (57) into Eq. (56). The result has the form

$$E - E_0 \sim -\frac{h^2}{J} \left(\frac{a}{R} \right)^{d-2}. \quad (58)$$

One can see that the highest energy gain is provided by spin adjustments at the atomic scale, $R \sim a$. In this case

one obtains

$$E - E_0 \sim -h^2/J. \quad (59)$$

Substituting R_f of Eq. (30) into Eq. (58), one recovers the IM energy of Eq. (31). One can see that the IM energy in the F-state is of the same order of magnitude as the regular IM energy. Because of the incomplete adjustment of spins to the random field in the F-state, one can expect that its IM energy contains a smaller numerical factor than Eq. (31). Nevertheless, this energy should be lower than Eq. (32) because of the logarithmic factor in the latter.

IX. MEMORY OF THE INITIAL CONDITION: ROTATIONAL ELASTICITY OF THE F-STATE

The magnetization in the F-state can be pointed in any direction because of the macroscopic isotropy of the problem. This direction practically coincides with the magnetization direction in the initial collinear state. Macroscopic isotropy does not mean, however, that the magnetization in the F-state can be freely rotated, as it can be in the isotropic ferromagnet. The reason is that the magnetization in the F-state is pinned by a partial adjustment to the random field. It has a memory of the initial collinear state. Rotation of the magnetization of the sample, even by a small angle, requires readjustment of the local magnetization that is inhibited by local energy barriers.

An illustration of this memory effect is the dependence of magnetization components on the magnetic field perpendicular to the initial magnetization shown in Fig. 18. The magnetization component in the direction of the field m_H increases from zero with a *finite slope* because of pinning, whereas the magnetization component along the initial magnetization m_m decreases to zero. After aligning with the field at larger fields, the magnitude of the magnetization increases. One can see Barkhausen jumps on the magnetization curves. For smaller or larger values of H_R the dependence m_H is less linear and it is difficult to scale results neatly.

Another, more pure, numerical experiment on the rotation of the magnetization in the F-state can be performed as follows. An F-state is prepared by the relaxation from a collinear state. Then a constrained energy minimization is performed with the magnetization direction fixed at the angle θ with its original direction.⁵² The value of θ is gradually increased from zero in both directions for the $3d\ xy$ model. The corresponding Lagrange multiplier is an adjustable magnetic field perpendicular to the instantaneous sample's magnetization. The results of this numerical experiment shown in Fig. 19 confirms strong pinning of the F-state. The magnetization does not rotate easily in the potential landscape created by the RF. Instead, it exhibits elasticity that can be interpreted as a memory of the initial state. While the energy

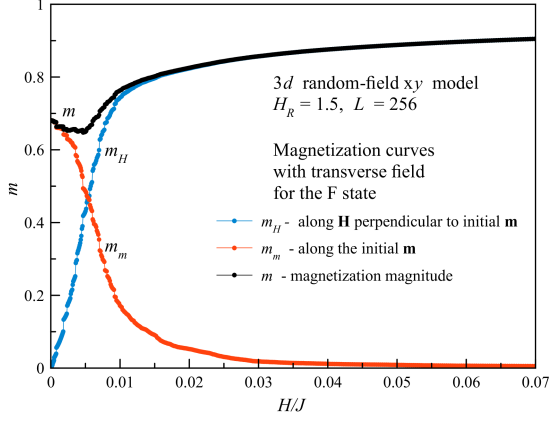


Figure 18: Magnetization curves of the F-state in the 3d xy model in transverse field.

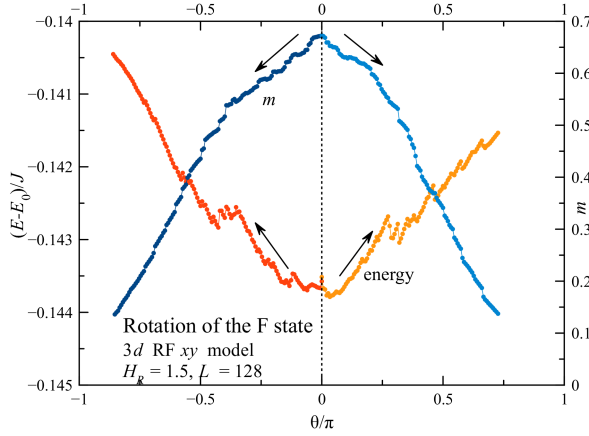


Figure 19: Rotation of the F-state.

increases for the rotation in any direction, the magnetization decreases to small values for which the method stops working.

X. EFFECTS OF TEMPERATURE

In this Section we consider effects of finite temperature with the help of the Monte Carlo Metropolis algorithm combined with over-relaxation. The relevant questions are whether the system orders spontaneously on cooling and whether finite temperature leads to the full disordering of the F-state by helping the system to overcome energy barriers.

The answer to the first question is negative. On cooling, the 3d xy system freezes into the vortex-glass (VG) state with a small magnetization being a finite-size effect. The energy of the VG state is higher than that of the F-state because of pinned vortex loops.² Numerical investigation shows that the VG state is not unique and depends on preparation. Relaxation from a random

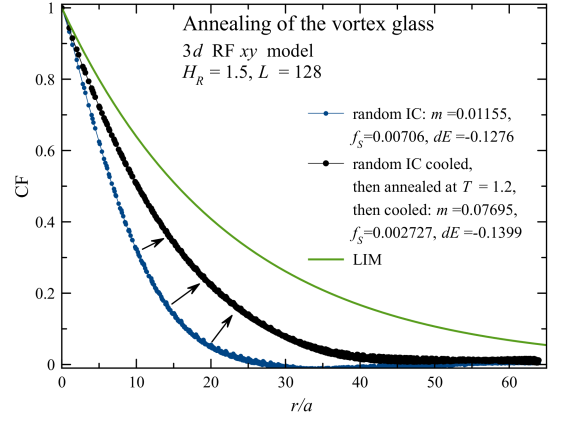


Figure 20: Annealing of the vortex-glass state.

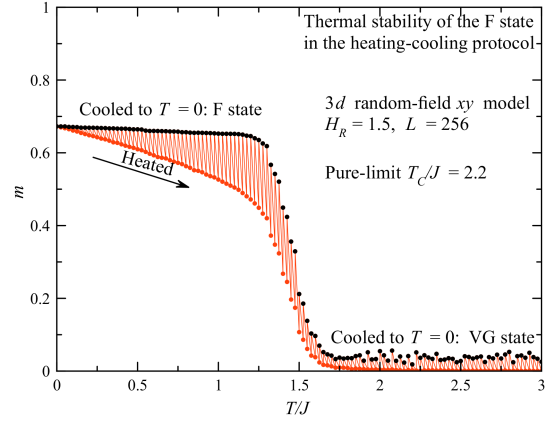


Figure 21: Heating-cooling protocol for 3d xy model. The temperature is increased in steps and each time dropped to zero.

state at $T = 0$, even using the algorithm with a slow energy loss, $\alpha \ll 1$, leads to the VG states with more vortices and higher energies. Stepwise lowering temperature leads to the VG states with less vortices and lower energies. As singularities in the spin field are breaking spin-spin correlations, the correlation functions of states with more singularities decay faster. To illustrate this point, annealing of the VG state of the 3d xy model with $H_R = 1.5$ obtained by relaxation from a random state at $T = 0$ has been done. After initial relaxation at $T = 0$, the temperature was raised to $T/J = 1.2$ and the system was equilibrated. After that the temperature was again dropped to zero. The obtained annealed state has lower vorticity and lower energy, while its correlation range is longer, as can be seen in Fig. 20. Annealing helps to depin and kill some vortex loops, while stronger pinned loops survive. Heating the system to even higher temperature would depin more vortex loops. However, this would create new ones. As a result, the annealing cannot eliminate vortex loops completely and it cannot bring the

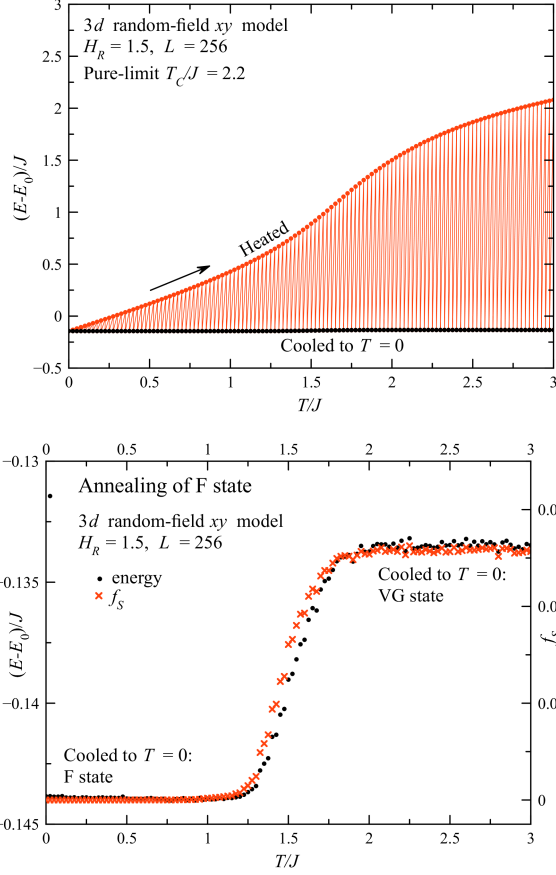


Figure 22: Energy in the heating-cooling protocol for 3d xy model. Lower panel: Magnification of the $T = 0$ results.

system from the VG state to the vortex-free state.

Next, we investigate thermal stability of the F-state by a heating protocol that consists of stepwise heating of the initial F-state to higher temperatures, each time allowing the system to relax at $T = 0$. The temperature sequence has the form $(0, T_1, 0, T_2, 0, T_3, \dots)$ with $T_1 < T_2 < T_3 \dots$. States with non-zero temperature are obtained with the Metropolis Monte Carlo routine, while zero-temperature states are obtained by the method of Ref. 2 that includes direct rotations of spins toward the effective field and over-relaxation. Since in this method the fraction of over-relaxation steps is dominant and the system is relaxing slowly, we do not call this sequence “annealing-quenching”. The magnetization results of this numerical experiment for the 3d xy model are shown in Fig. 21. For the temperatures below $1.2J$, the system returns to the F-states. Heating to higher temperatures creates vortex loops that get pinned and do not collapse upon dropping T to zero. Thus the F-state gets destroyed by heating to higher temperatures, the resulting state being the VG state.

The energy in the heating-cooling protocol is shown in Fig. 22. In the upper panel, the non-zero-temperature branch looks familiar with the largest slope (the maxi-

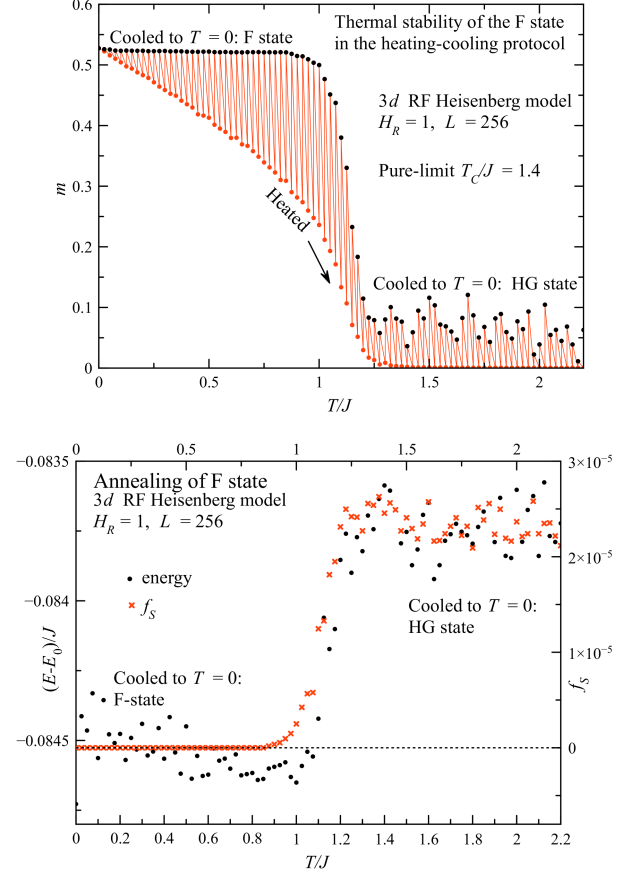


Figure 23: Heating-cooling protocol for 3d Heisenberg model. Lower panel: energy and singularity fraction at $T = 0$.

um of the heat capacity) around $T/J = 1.6$ for $H_R/J = 1.5$ used here. For the pure model there is a ferromagnetic phase transition at $T/J = 2.2$. The $T = 0$ branch on the upper panel looks as a straight line. However, the magnification in the lower panel shows a fine structure with transition from the F-state to the higher-energy VG state above $T/J = 1.2$. In fact, there is a crossover from the F to VG state. The excessive energy of the VG state perfectly correlates with the fraction of singularities.²

We also have performed the heating-cooling experiment for a 3d Heisenberg model. The results shown in Fig. 23 are similar to those for the xy model above. Since hedgehogs in the Heisenberg model carry much less energy than the vortex loops in the xy model, the energy of the hedgehog-glass (HG) is only slightly above that of the F-state.

XI. DISCUSSION AND CONCLUSIONS

We have presented a comparative study of glassy states of three-dimensional xy and Heisenberg random-field models. The xy spin model is conceptually similar to the

model of a pinned flux lattice, even though the symmetry of the two models is slightly different.⁴² The Heisenberg RF model has practical implementation in antiferromagnets with quenched disorder.¹⁴ Some of the properties of the two models may be also relevant to properties of amorphous and sintered magnets, although there are very significant differences between the effects of the random field and random anisotropy.

Earlier we have found that the properties of the random-field model are controlled by topology.¹ For the n -component spin in d dimensions the reversible behavior with exponential decay of correlations occurs at $n > d+1$ when topological defects are absent. At $n \leq d$ the random-field system possesses pinned topological defects and exhibits glassy behavior. The focus of this paper has been on the properties of the F-state obtained by relaxation from the initially ordered state. One of our main findings is a profound difference between the F-states of the xy model and the Heisenberg model. While the latter can easily be transformed into a lower energy state with $m = 0$ by applying an appropriate hysteresis cycle, the xy F-state appears robust against attempts to lower its energy and decrease the magnetization at the same time. This can be traced to the inevitable presence of topological defects in the $m = 0$ state at $n \leq d$.^{1,2} In the $3d$ Heisenberg model such defects are hedgehogs that have relatively low energy as compared to the vortex loops in the $3d$ xy model. It is the reluctance of the xy RF system to form high-energy vortex loops that makes the F-state robust with respect to disordering.

Our other interesting finding is that the F-state possesses memory of the initial state. There is an infinite number of F-states that differ from each other by the direction of the global magnetic moment determined by the initial ordered state that the F-state has evolved from. Unlike in a ferromagnet with the exchange interaction only, these states are separated by energy barriers due to the random field. Small rotation of the magnetization of the F-state reveals its elasticity: rotation generates forces that return \mathbf{m} to its original direction. This makes one wonder whether the F-state has any relevance to the elastic glass discussed in the past.^{30,38}

We have also studied the effect of temperature on the F-state. Naively, one would expect that it can be easily annealed towards thermal equilibrium. Our results do not support this expectation. While heating helps to depin topological defects, it also creates the new ones. Annealing of the vortex glass state does result in the lower vorticity and lower energy but it cannot eliminate vortices completely. On the contrary, heating and cooling of the F-state generates vortex loops that have been completely absent at the beginning. This reduces the magnetization but also leads to the higher energy than the energy of the F-state not subjected to the heating-cooling procedure. The bottom line is that the RF system, when cooled down after exposure to elevated temperature, behaves as a glass. It stores the thermal energy in the form of pinned topological defects.

There is a deep analogy between this state and the state of a conventional bulk ferromagnet with defects. In the case of the conventional ferromagnet the magnetization and the internal dipolar field adjust self-consistently through equations of magnetostatics. In a similar manner, the magnetization of the RF system adjusts self-consistently to the average random field. When cooled in a zero field below the Curie temperature, a conventional ferromagnet ends up in a state with small domains and high energy dominated by pinned domain walls. Similarly, the RF magnet ends up with many pinned topological defects: vortex loops in the xy model and hedgehogs in the Heisenberg model. When relaxing from a magnetized state at a sufficiently low temperature, a conventional ferromagnet ends up in a state with a finite magnetization because domain walls cannot easily penetrate in the magnet due to pinning and, thus, cannot form the $m = 0$ ground state. In a similar manner, the RF magnet ends up in the F-state when it relaxes from the ordered initial state. There are significant differences though as well. The $m = 0$ ground state of a conventional ferromagnet is the minimum of magnetostatic energy that has not been considered in the context of the RF system studied by us and by other authors. It is not at all obvious whether the xy system in the F-state can lower its energy by accommodating a large vortex loop that would reduce the magnetization to zero. Although there may be little profit in discussing the ground state of the glassy system, some remarks are in order.

The Imry-Ma argument is clearly qualitatively valid as long as the $m = 0$ state does not require topological defects.¹ At $n \leq d$ the argument becomes less obvious as the IM domains cannot be formed without topological defects. On the first glance, it appears that topological defects only modify the IM argument but do not destroy it. Indeed, in $3d$ there would be roughly one vortex loop per IM domain of size R . The energy of the loop would be of order $2\pi Js^2(R/a) \ln(R/a)$, that corresponds to the energy $2\pi Js^2(a/R)^2 \ln(R/a)$ per spin. This modifies the exchange energy in Eq. (29) by a factor proportional to $\log(R)$ and leads to a greater but still finite R_f in the disordered state. Finally, the energy gain of the IM state becomes strongly reduced, see Eq. (32). At the same time, the IM energy in the vortex-free F-state of the $3d$ xy model, see Eq. (56) and below, remains of the same order as the regular IM energy of Eq. (31).

For the $3d$ Heisenberg model, the energy of a hedgehog in the domain of size R is $4\pi Js^2(R/a)$, which modifies the exchange energy per spin and the resulting IM energy by a factor of order unity. Thus estimations for the energies of the disordered states and the F-states are the same. Making hysteresis loops with decreasing amplitude converts the F-state into a disordered state of a lower energy. This indicates that the ground state of the $3d$ Heisenberg model may be disordered in spite of hedgehogs.

One should note that in the presence of topological defects the IM argument becomes less precise as it ignores misalignment of the spin field with the average random

field due to defects, as well as the interaction between topological defects. There is also a scaling argument that makes the IM argument even less obvious. Indeed, the IM argument relies on the large size of IM domains in which the direction of the magnetization follows the RF field averaged over the volume of the domain. It implies smooth rotation of the magnetization from one domain to the other. The argument would not apply to the case in which the RF field h at each site of a $3d$ cubic lattice is of the order of the exchange field $6Js$ created by the neighboring spins, because it would be difficult to say without direct computation whether the effect of the RF would win over the effect of the exchange. In this connection, one should notice that by considering blocks of spins of size r satisfying $a < r < R_f$, the original problem described by the Hamiltonian (2) can be rescaled to the problem described by the same Hamiltonian with the rescaled $s_r = s(r/a)^3$, $J_r = J(a/r)^5$, and $h_r = h(a/r)^{3/2}$. This gives the same expression for the correlation length, $R_f/r = (2\pi/9)(1 - 1/n)^{-1}(6J_r s_r/h_r)^2$. For the blocks of size $r \sim R_f$ one has $h_r \sim 6J_r s_r$ in the rescaled problem. This shows that the existence of a small parameter

$h/(6J)$ in the original problem with weak RF may be an illusion. The original problem with $h \ll 6Js$ is mathematically equivalent to the rescaled problem in which the local exchange field and the RF field are of the same order of magnitude. At $h \gg 6Js$ the spins obviously align with the RF, yielding the state with $m = 0$. The question, therefore, is whether decreasing h from $h \gg 6J$ would result in the bifurcation or the ground state to a non-zero m at some $h \sim 6Js$. This is suggested by Figs. 10 and 11. The answer for the ground state may depend on the number of spin components n . However, looking for the ground state in a glassy system requires a different numerical algorithm based on the global energy minimization. Whether this is worth the effort is another question.

XII. ACKNOWLEDGEMENTS

This work has been supported by the U.S. Department of Energy through Grant No. DE-FG02-93ER45487.

-
- ¹ T. C. Proctor, D. A. Garanin, and E. M. Chudnovsky, Phys. Rev. Lett. **112**, 097201 (2014).
 - ² D. A. Garanin, E. M. Chudnovsky, and T. Proctor, Phys. Rev. B **88**, 224418 (2013).
 - ³ A. I. Larkin, Sov. Phys. JETP **31**, 784 (1970).
 - ⁴ G. Blatter, M. V. Feigel'man, V. B. Geshkenbein, A.I. Larkin, and V. M. Vinokur, Rev. Mod. Phys. **66**, 1125 (1994).
 - ⁵ Y. Imry and S.-k. Ma, Phys. Rev. Lett. **35**, 1399 (1975).
 - ⁶ M. Aizenman and J. Wehr, Phys. Rev. Lett. **62**, 2503 (1989).
 - ⁷ M. Aizenman and J. Wehr, Commun. Math. Phys. **130**, 489 (1990).
 - ⁸ E.M. Chudnovsky and R.A. Serota, Phys. Rev. B **26**, 2697 (1982).
 - ⁹ R. Pelcovits, E. Pytte, and J. Rudnick, Phys. Rev. Lett. **40**, 476 (1978).
 - ¹⁰ J. D. Patterson, G. R. Grusalski, and D. J. Sellmyer, Phys. Rev. B **18**, 1377 (1978).
 - ¹¹ A. Aharony and E. Pytte, Phys. Rev. Lett. **45**, 1583 (1980).
 - ¹² D. S. Fisher, Phys. Rev. B **31**, 7233 (1985).
 - ¹³ See, e.g., E. M. Chudnovsky, W. M. Saslow and R. A. Serota, Phys. Rev. B **33**, 251 (1986), and references therein.
 - ¹⁴ S. Fishman and A. Aharony, J. Phys. C: Solid State Phys. **12**, L729 (1979).
 - ¹⁵ K. Binder and A. P. Young, Rev. Mod. Phys. **58**, 801 (1986).
 - ¹⁶ R. Seshadri and R.M. Westervelt, Phys. Rev. B **46**, 5142 (1992); *ibid.* **46**, 5150 (1992).
 - ¹⁷ E. M. Chudnovsky, Phys. Rev. B **43**, 7831 (1991).
 - ¹⁸ K. B. Efetov and A. I. Larkin, Sov. Phys. JETP **72**, 2350 (1977).
 - ¹⁹ T. Bellini, N. A. Clark, V. Degiorgio, F. Mantegazza, and G. Natale, Phys. Rev. E **57**, 2996 (1998).
 - ²⁰ E. M. Chudnovsky, Phys. Rev. Lett. **103**, 137001 (2009).
 - ²¹ G. E. Volovik, J. Low Temp. Phys. **150**, 453 (2008).
 - ²² J. I. A. Li, J. Pollanen, A. M. Zimmerman, C. A. Collett, W. J. Gannon, and W. P. Halperin, Nat. Phys. **9**, 775 (2013).
 - ²³ J. L. Cardy and S. Ostlund, Phys. Rev. B **25**, 6899 (1982).
 - ²⁴ J. Villain and J. F. Fernandez, Z. Phys. B - Condens. Matter **54**, 139 (1984).
 - ²⁵ T. Nattermann, Phys. Rev. Lett. **64**, 2454 (1990).
 - ²⁶ J. Kierfield, T. Nattermann, and T. Hwa, Phys. Rev. B **55**, 626 (1997).
 - ²⁷ S. E. Korshunov, Phys. Rev. B **48**, 3969 (1993).
 - ²⁸ T. Giamarchi and P. Le Doussal, Phys. Rev. Lett. **72**, 1530 (1994).
 - ²⁹ T. Giamarchi and P. Le Doussal, Phys. Rev. B **52**, 1242 (1995).
 - ³⁰ See, e.g., T. Nattermann and S. Scheidl, Adv. of Phys. **49**, 607 (2000), and references therein.
 - ³¹ D. E. Feldman, Phys. Rev. B **61**, 382 (2000).
 - ³² P. Le Doussal and K. J. Wiese, Phys. Rev. Lett. **96**, 197202 (2006).
 - ³³ P. Le Doussal, Phys. Rev. Lett. **96**, 235702 (2006).
 - ³⁴ A. A. Middleton, P. Le Doussal, and K. J. Wiese, Phys. Rev. Lett. **98**, 155701 (2007).
 - ³⁵ S. Bogner, T. Emig, A. Taha, and C. Zeng, Phys. Rev. B **69**, 104420 (2004).
 - ³⁶ H. Orland and Y. Shapir, Europhys. Lett. **30**, 203 (1995).
 - ³⁷ T. Garel, G. Lori, and H. Orland, Phys. Rev. B **53**, R2941 (1996).
 - ³⁸ D. Fisher, Phys. Rev. Lett. **78**, 1964 (1997).
 - ³⁹ R. Dickman and E. M. Chudnovsky, Phys. Rev. B **44**, 4397 (1991).
 - ⁴⁰ B. Dienes and B. Barbara, Phys. Rev. B **41**, 11549 (1990).
 - ⁴¹ R. Fisch, Phys. Rev. B **52**, 12512 (1995); *ibid.* **55**, 8211

- (1997); *ibid* **57**, 269 (1998); *ibid* **62**, 361 (2000); *ibid* **76**, 214435 (2007); *ibid* **79**, 214429 (2009).
- ⁴² M. J. P. Gingras and D. A. Huse, *Phys. Rev. B* **53**, 15193 (1996).
- ⁴³ D. A. Garanin, E. M. Chudnovsky, and T. Proctor, *Europhys. Lett.* **103**, 67009 (2013).
- ⁴⁴ C. Zeng, P. L. Leath, and D. S. Fisher, *Phys. Rev. Lett.* **82**, 1935 (1999).
- ⁴⁵ A. Perret, Z. Ristivojevic, P. Le Doussal, G. Schehr, and K. J. Wiese, *Phys. Rev. Lett.* **109**, 157205 (2012).
- ⁴⁶ C. Zeng, A. A. Middleton, and Y. Shapir, *Phys. Rev. Lett.* **77**, 3204 (1996).
- ⁴⁷ H. Rieger and U. Blasum, *Phys. Rev. B* **55**, R7394 (1997).
- ⁴⁸ M. Itakura, *Phys. Rev. B* **68**, 100405(R) (2003).
- ⁴⁹ M. Itakura and C. Arakawa, *Prog. Theor. Phys. Suppl. No.* **157**, 136 (2005).
- ⁵⁰ T. Klein, I. Joumard, S. Blanchard, J. Marcus, R. Cubitt, T. Giamarchi, and P. Le Doussal, *Nature* **413**, 404 (2001).
- ⁵¹ H. E. Stanley, *Phys. Rev.* **176**, 718 (1968).
- ⁵² D. A. Garanin and H. Kachkachi, *Phys. Rev. Lett.* **90**, 65504 (2003).